J. Korean Soc. Combust. 21(4) (2016) 16-22

〈학술논문〉 DOI: https://doi.org/10.15231/jksc.2016.21.4.016 ISSN 1226-0959
eISSN 2466-2089

충격파관 저압실/고압실 직경비에 따른 압력변동에 대한 수치해석

왕위엔강[*] · 김철진[*,**] · 손채훈[*†] · 정인석[***]

[*]세종대학교 기계공학과 · [**]호원대학교 국방과학기술학과 · [***]서울대학교 항공우주공학과

A Numerical Study on Pressure Variation in a Shock Tube by Changing the Diameter Ratio of Low-Pressure (Driven) to High-Pressure (Driver) Part

YuanGang Wang[*], Chul Jin Kim[*,**], Chae Hoon Sohn[*†] and In-Seuck Jeung[***]

[*]Department of Mechanical Engineering, Sejong University
[**]Department of Defence Science & Technology, Howon University
[***]Department of Aerospace Engineering, Seoul National University

(Received 1 September 2016, Received in revised form 12 October 2016, Accepted 12 October 2016)

ABSTRACT

Pressure and temperature variations in a shock tube have been studied numerically by changing the diameter ratio of a driven part to a driver part . There are five cases where the adopted diameter ratios are 40%, 50%, 60%, 80%, and 100% respectively. The diameter of the driver part remains unchanged meanwhile the shock tube driven part diameter increases from 40% to 100% of the driver part. In the 100% ratio case, the driver part and driven parts have the same diameter of 66.9 mm. As the diameter ratio decreases, the pressure in the shock tube and available test time are increased.

Key Words : Shock tube, Driven part, Driver part, Available test time

1. Introduction

As the research focuses on combustion process in internal combustion engine move along, the chemical kinetic mechanisms of various hydrocarbon fuels need to be verified by their ignition delay time at different temperature and pressure during the combustion process. Based on ignition delay time analysis and research, it can provide important theoretical support for new combustion technologies, design improvements of the combustion chamber, increase in combustion efficiency, and reduction of pollutant emission [1].

Shock tube is the experimental device that uses the principle of gas compression to achieve very high stagnation temperatures. Temperature, pressure, and shock speed can be easily adjusted over a wide range by using the incident and reflected shocks in the tube. So, the shock tube is a useful device to study the ignition delay time and chemical kinetics. And, it has been widely used in the related field [2].

Ignition and extinction has been studied for understanding of transient phenomena [3]. Researches about ignition delay time and chemical kinetics have been developed for a long time by using shock tube and the approaches are well known [4,5]. For this research, first, a shock tube is designed, manufactured, and tested to measure ignition delay time of a mixture of fuel and oxidizer. But, before manufacturing, we need to check on whether shock tube can provide desirous conditions of pressure and temperature or not. That is, we have to set up an initial condition specified by pressure and temperature.

A shock tube is composed of a high pressure or

† Corresponding Author, chsohn@sejong.ac.kr

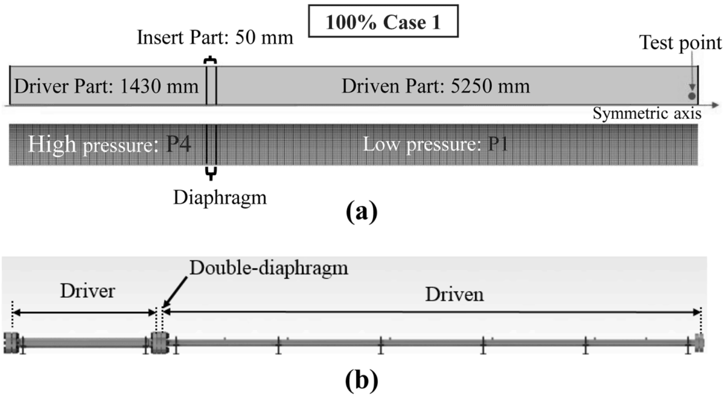

Fig. 1. The structure and dimension of the shock tube.

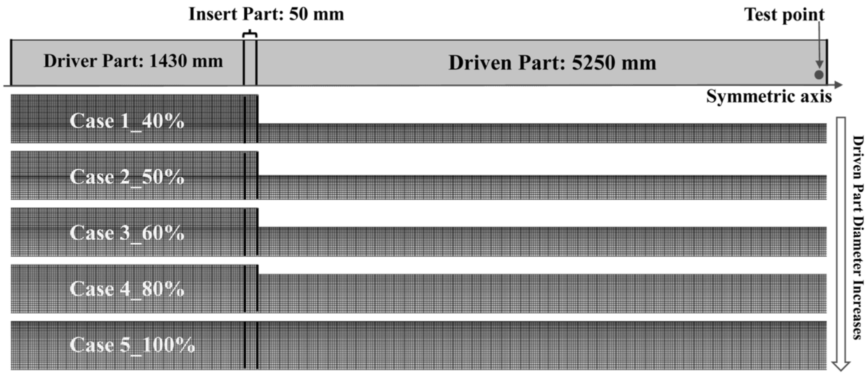

Fig. 2. Geometries of the driver and driven parts (upper half only) of the shock tube ranging from the diameter ratio of 40% to 100% in 5 cases.

driver part and a low pressure or driven part which are separated by an insert which plays the role of diaphragm. The geometry of a shock tube is illustrated in Fig. 1(a). In numerical simulations, it is a 2D axisymmetric model and meshed by the structured grids. The driver and the driven parts have lengths of 1430 mm and 5250 mm, respectively. The insert with the length of 50 mm is used to replace the function of double-diaphragm. Fig. 1(b) shows a shock tube which is designed to conduct an experiment in our group [6]. The numerical analysis will be done by this shock tube.

In the present paper, the purpose is that we investigate the influence of the shock tube dimension on pressure, temperature and available test time by changing the diameter ratio of the driven part to the driver part. Fig. 2 shows geometries of the driver and the driven parts diameter in 5 cases, where the diameter ratio ranges from 40% to 100% and the driver part remains unchanged. The diameter ratios of the 5 cases are 40%, 50%, 60%, 80%, and 100%, respectively. And, 5 cases are named from Case 1 to Case 5. As the driven part is changed, the number of the mesh grids varies from 130,000 to 230,000 with the same structured mesh method. To check the grid-independency, two other cases were considered for simulation with 300,000 and 470,000 grids and the results showed no significant variation [7]. The detailed information of the driven part diameters and mesh grids in 5 cases are listed in Table 1.

Table 1. The driven part diameter and mesh grids variation of 5 cases

Case	Driver part diameter [mm]	Driven part diameter [mm]	# of Mesh grids
Case1_40%	66.9	26.76	130,000
Case2_50%	66.9	33.45	150,000
Case3_60%	66.9	40.14	166,000
Case4_80%	66.9	53.52	170,000
Case5_100%	66.9	66.90	230,000

2. Numerical Methods

2.1. Governing Equations

For the numerical analysis of internal flow in the shock tube, the following governing equations are solved:

continuity equation,

$$\frac{\partial}{\partial t}(\rho)+\nabla \cdot (\rho\vec{v})=S_m, \quad (1)$$

momentum equation,

$$\frac{\partial}{\partial t}(\rho\vec{v})+\nabla \cdot (\rho\vec{v}\vec{v})= -\nabla p+\nabla \cdot (\bar{\bar{\tau}})+\rho\vec{g}+\vec{F}, \quad (2)$$

energy equation,

$$\frac{\partial}{\partial t}(\rho E)+\nabla \cdot (\vec{v}(\rho E+p))= \nabla \cdot \left(k_{eff}\nabla T-\Sigma_j h_j\vec{j}_j+\left(\bar{\bar{\tau}}_{eff}\cdot\vec{v}\right)\right)+S_h, \quad (3)$$

and finally, equation of state,

$$\rho=\frac{(p+p_{ref})M_w}{RT}. \quad (4)$$

To simulate formation and propagation of shock wave, the above equations of Eqs. (1)-(3) are transformed to Reynolds-averaged Navier-Stokes (RANS) equations. In the present flow, viscosity effect is significant near the tube wall. And, the Navier-Stokes equation is solved with a RANS model instead of solving the Euler equation. The RANS equations are solved simultaneously with the aid of appropriate numerical schemes and all simulations are calculated by using the general purpose CFD code, FLUENT [8]. Of various turbulent flow models, the SST(Shear Stress Transport) k-ω turbulent model is adopted in this study. Because this model is more accurate and reliable for supersonic flows [9]. For spatial discretization of the partial differential equations, the 2nd-order upwind scheme is employed. And, transient flow is solved with the density-based scheme and time integration. The time step for simulation is 5×10^{-7} sec. The time interval is sufficiently short to get reliable results. Two cases with time steps of 1×10^{-6} and 4×10^{-7} were tested and the results showed slight errors between them.

2.2. The basic concept of shock tube

The principle and concept to measure ignition delay time with shock tube are illustrated in Fig. 3. As shown in the figure, there are 3 main stages during the shock tube experiment. At the first stage, the driver part is filled with high pressure gas and the driven part is filled with low pressure gas of which ignition delay time will be measured. When high pressure driver gas expands upon breaking the diaphragm, the shock wave will be generated. The shock wave moves to the right end plate and in the meanwhile, it compresses the low pressure gas in the driven part [11]. At this stage, the

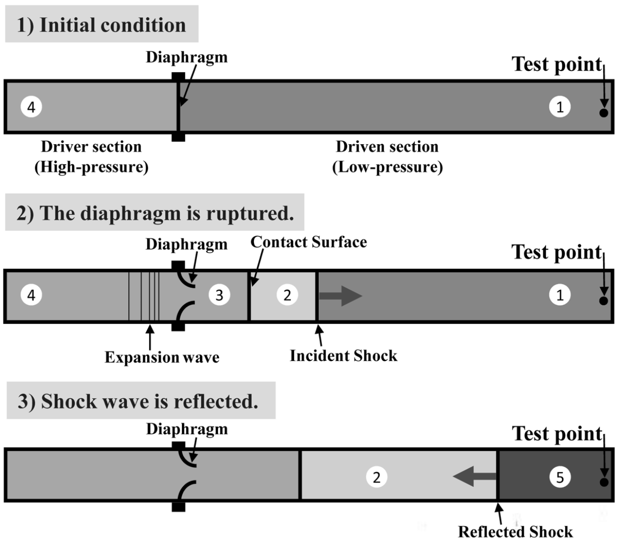

Fig. 3. Three stages of shock tube operation and the area serial number assigned [10].

Table 2. The zone number, its position, and notations for pressure and temperature

Area	Position	Pressure	Temperature
①	Driven part	P1	T1
②	Behind the incident shock	P2	T2
③	Behind the contact surface	P3	T3
④	Driver part	P4	T4
⑤	Behind the reflected shock	P5	T5
...	...	...	...

low pressure gas area still unaffected by shock wave in the driven part is named as Zone 1. And, the initial high gas area in the driver part is called Zone 4. At the second stage of shock wave propagation, the zone behind the incident shock is named as Zone 2. The area behind the contact surface is named as Zone 3. The surface between Zones 2 and 3 is the contact surface. After the incident shock arrives at the end plate, it is reflected by the end wall and the reflected shock is formed at the third stage. And, the volume behind the reflected shock is named as Zone 5. The zone number and each position of these 5 zones are listed in Table 2. And, their notations for pressure and temperature also can be seen from the table. Actually, in the shock tube, there are not just 5 zones, but more zones after the diaphragm is ruptured and the reflected shock is generated. In this paper, the 5 zones are focused to explain this study.

During the third stage, the low pressure gas (tested gas) is instantaneously compressed and heated to high temperature by the incident shock first and then, by the reflected shock again, leading to higher temperature, which corresponds to the final-state temperature and at the same time, the intial temperature for ignition simulation. The gas flow in Zone 2 is behind the incident shock, which has quite high mach number. Some studies related to gas dynamics can be carried out by utilizing the gas flow in this zone. In Zone 5, the gas flow is behind the reflected shock wave. The gas in this zone is compressed twice by the incident and reflected shocks. It has the features of elevated temperature and high pressure which is suitable for various experimental studies including ignition delay time measurement. The temperature and pressure in Zone 5 have the wide ranges of 600-4000 K and 0.1-

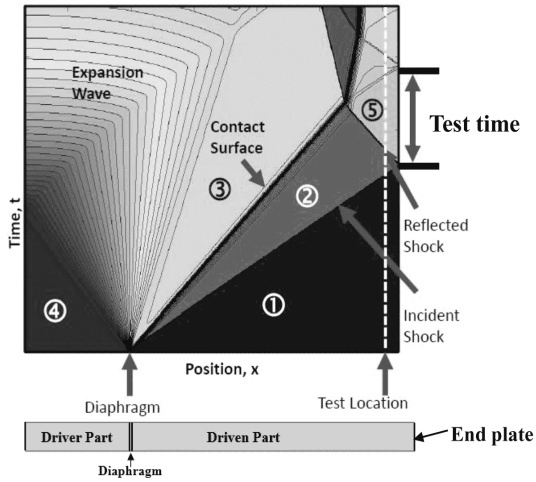

Fig. 4. The schematic of the behavior in the shock tube after the diaphragm is ruptured [10].

1000 atm, respectively [2]. The shock tube which adopts the gas in Zone 5 as the research target is called a chemical shock tube or a reflective shock tube. That is, the purpose is to measure the ignition delay time of test fuel in Zone 5 by using this tube [12,13].

From Fig. 4, we can understand the behavior in the shock tube graphically after the incident shock is generated. As aforementioned, when the diaphragm is broken, the incident shock is generated and moves to Zone 1. The expansion wave moves to Zone 4. When the incident shock reaches the end plate, it is reflected and the reflected shock is generated. Then, the reflected shock moves to the contact surface which is the interface between Zones 2 and 3 and it interacts with the contact surface. A key parameter is introduced here, which is the test time available for measurement of ignition delay time. As shown in Fig. 4, the test time is defined as time taken from generation of the reflected shock till its interaction with the contact surface. That is, during the test time, the mixture gas in Zone 5 keeps constant temperature and pressure, which are initial temperature and pressure, respectively.

To design the shock tube to be used for measurement of ignition delay time of a mixture, the available test time must be calculated firstly. In this work, it is calculated by considering non-reactive flow field in the shock tube. After the test time is obtained from the non-reactive flow in a certain tube, we can compare it with the ignition delay time reported in previous works to see that whether the shock tube can be used to measure the ignition delay time or not. The longer test time is, the more flexible fuel can be tested by the shock tube. Accordingly, in this work, we adopt the non-reactive flow and change the diameter ratio of driven to driver parts of the shock tube to check the effect of the ratio on test time as well as pressure and temperature in Zone 5. Then, we can find how to increase the test time.

2.3. The Initial Conditions

In this numerical study, chemical reaction is not considered in the shock tube because the available test time is calculated at the design stage of a shock tube. The high pressure or driver part is filled with nitrogen as the driver gas and air as the low pressure gas in the driven part. The combination of nitrogen and air is selected for comparative study with our future experimental work. As an initial condition, the pressures in driver and driven parts, which are named as P4 and P1, respectively, are set to be 30 atm and 1 atm, respectively. Initial gas temperature in the entire shock tube is 300 K. This means that the initial conditions are the same in all the 5 cases and the only variable is the diameter of the driven part. And, a test or monitoring point designated to check the state in Zone 5 is placed near the end plate as shown in Fig. 1.

3. Numerical Results

Numerical simulations for the 5 cases are conducted and pressure fields are demonstrated in Fig. 5, where the incident shocks (a) and reflected shocks (b) can be identified by the pressure contours in the driven parts in the 5 cases. The pressure contour is illustrated in a part ranging from the location of 3 m to that of 5.3 m in the driven part. Fig. 5(a) shows the pressure contours in the 5 cases at the time lapse of 6 ms after the incident shock is generated. From the figures, the light blue Zone 2 and the dark blue Zone 1 can be seen clearly in each case. The boundary between the two zones means the boundary between the high and the low pressure gases. This line is also regarded as the incident shock wave. At the same time lapse of 6 ms after the incident shock wave is generated, the shock positions are different from each other in the cases, where the diameter ratio increases from 40% to 100%. The shock wave is the closest to the end plate of the 5 cases. That means that the shock speed in the case 1, where the diameter ratio is the smallest or 40%, has the fastest speed of the 5 cases. As the diameter ratio increases, the shock speed decreases. Similarly, the pressure contour in Fig. 5 (b) shows propagation of the reflected shock wave. In this figure, the left light Zone 2 and the right Zone 5 are seen and the boundary between the two zones corresponds to the reflected shock wave. The reflected shock in the case 1 has the fastest speed. By comparing the 5 cases at the same time lapse of 12 ms, it is found that the shock speed decreases as the diameter ratio increases from case 1 to case 5.

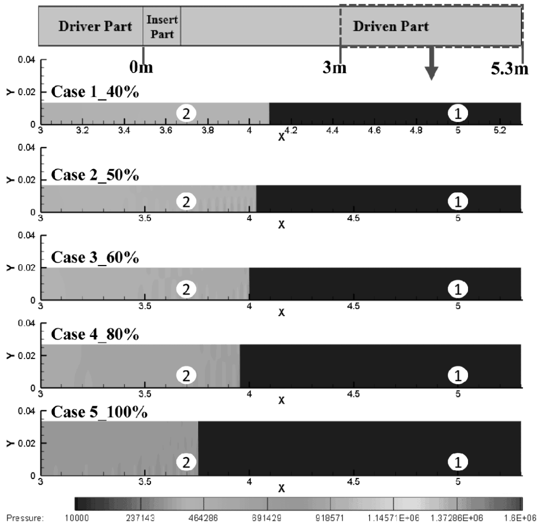

(a) t = 6 ms

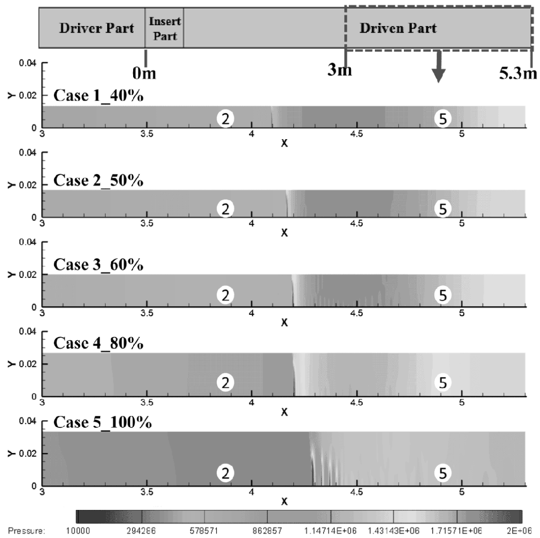

(b) t = 12 ms

Fig. 5. Pressure fields of incident shock (a) and reflected shock (b) in 5 cases.

In Fig. 6, the pressure variation in time can be seen clearly in the 5 cases. The first abrupt pressure rise appears between 7.5 ms and 8.5 ms in the 5 cases with the same order as diameter ratio increases. This pressure rise is caused by passage of the incident shock. And, the ascending order of 5 cases in time is consistent with the descending order of the incident shock speed. After the first rise, the pressure remains constant for a short time and then, the second sudden rise appears. This is because the incident shock is reflected at the Fend plate and the gas is compressed again. After the second rise, the pressure remains nearly constant for a long time with small fluctuations. As seen in Fig. 3, the pressure during this period is denoted by P5, i.e., pressure in Zone 5. Duration during the period means available test time as shown in Fig. 4.

In Fig. 7, the similar behaviors of temperature to those of the pressure shown in Fig. 6 are shown. The temporal profiles of temperature also show two abrupt changes, which are caused by the incident shock first and the reflected shock secondly. During the test time, the temperature in each case remain constant, which is called T5 as explained in Fig. 3 and Table 2. From this figure, the T5 also shows the ascending order from case 1 to case 5.

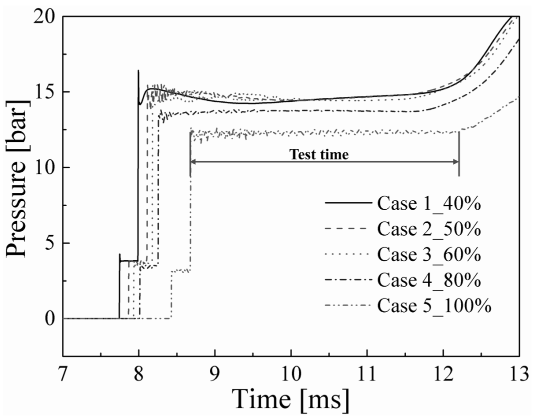

Fig. 6. The pressure variation on the test point and the measuring of test time.

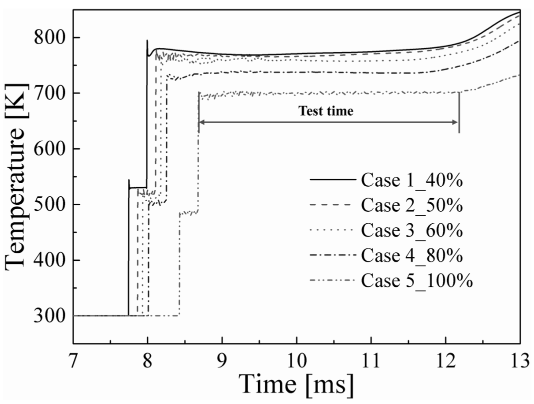

Fig. 7. The temperature variation on the test point of 5 cases.

From Figs. 6 and 7, the P5 and T5 in the 5 cases are compared with each other and shown in Fig. 8. And, Fig. 8 also illustrates the comparison of available test time and Mach number in the 5 cases. All the data are normalized by each value in case 5. Detailed numerical results are listed in Table 3. To better understand the variation trend as the driven part diameter increases, the driven part aspect ratios are calculated and shown in Table 3. The horizontal axis of Fig. 8 is set to be aspect ratio of the driven part. All the variables show the same decreasing trend as the driven part aspect ratio increases. It is found that the T5, P5, test time, and Mach number in Zone 5, which is selected as initial volume of the mixture, can be increased by decreasing the diameter of driven part. Additionally, the effect of density ratio on test time is also studied although not shown here. The density ratio means the ratio of driver

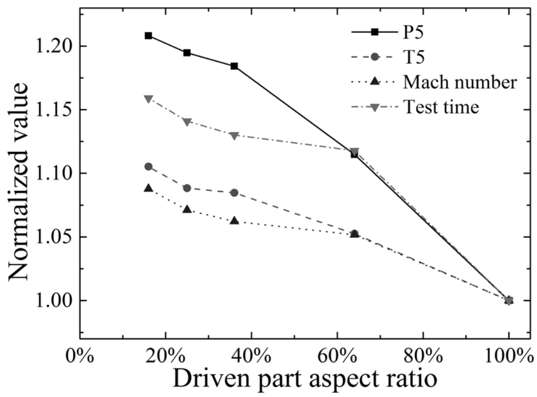

Fig. 8. The variation of P5, T5, Mach number and Test time of 5 cases.

Table 3. The values of P5, T5, Mach number, and test time in the 5 cases.

Case	Aspect ratio	P5 [bar]	T5 [K]	Mach No.	Test time [ms]
Case1_40%	16%	14.85	773	1.99	4.18
Case2_50%	25%	14.68	761	1.96	4.12
Case3_60%	36%	14.55	758	1.95	4.08
Case4_80%	64%	13.70	736	1.93	4.03
Case5_100%	100%	12.29	700	1.83	3.61

part gas density to driven part gas density. It is found that the test time increases with the density ratio.

4. Conclusion

In this paper, a numerical study on pressure, temperature, test time, and Mach number variation in a shock tube by changing the diameter ratio of a driven part to a driver part has been conducted. When the diameter ratio increases from 40% to 100%, the incident shock speed decreases leading to decrease in Mach number. And, the pressure, temperature, and available test time generated by the reflected shock wave decrease as well. It indicates that the condition, especially test time, made by the reflected shock wave can be controlled by changing the diameter ratio of a driven and driver parts of a shock tube.

In our future work, the test time predicted with our shock tube will be compared with the ignition delay time which has been reported in the previous works to verify the availability of our shock tube in the development stage. And then, the shock tube will be used to measure ignition delay time of target fuels.

Acknowledgement

본 연구는 서울대학교 차세대 우주추진 연구센터와 연계된 미래창조과학부의 재원으로 한국연구재단의 지원을 받아 수행한 선도연구센터지원사업(NRF-2013R1A5A1073861)의 연구 결과입니다. 또한, 본 연구에서 저자중 손채훈은 한국연구재단(미래창조과학부)의 우주핵심기술개발사업(NRF-2015M1A3A3A02009957)에 의해 지원을 받았으며, 이에 감사드립니다.

References

[1] Phipippe Dagaut, On the kinetics of hydroncarbons oxidation from natural gas to kerosene and diesel fuel, Phys. Chem. Chem. Phys, 2002, 2079-2094.

[2] NanBei, The Development of High Pressure Shock Tube and Experimental Study on Ignition Delay of Hydrocarbon, Shanghai jiaotong University, Master's thesis, 2011, 2-7.

[3] Tae Hyung Kim, Oh Boong Kwon, Jeong Park, Sang-In Keel, Jin-Han Yun and Jong Ho Park, A Study on Flame Extinction in Oxymethane Combustion, J. Korean Soc. Combust., 20 (2015), 34-41.

[4] Robert S. Tranter, Binod R. Giri and John H. Kiefer, Shock tube/time-of-flight mass spectrometer for high temperature kinetic studies, Review of scientific instruments, 78 (2007), No. 034101.

[5] A. E.L. Bakali, P. Dagaut, L. Pillier and P. Meunier, Experimental and modeling study of the oxidation of natural gas in a premixed flame, shock tube, and jet-stirred reactor, Combustion and Flame, 137 (2004), 109-128.

[6] William Adolph Crede, The design and construction of a shock tube facility, Missouri university of science and technology, Master's thesis, 1965.

[7] Amrollah Moradi, Fata Mohammadi Fard, Mahmoud Mani, Mohamadali Ranjbar, Mobin Mottaghipour, "Experimental and numerical investigation of AUT shock tube", European Journal of Experimental Biology, 2 (2012), 1820-1826.

[8] ANSYS Inc., ANSYS Fluent Theory Guide, 2015.

[9] Y. Bartosiewicz, Zine Aidoun, P. Desevaux, Y ves Mercadier, Numerical and experimental investigations on supersonic ejectors, International Journal of Heat and Fluid Flow, 26 (2005), 56-70.

[10] Ronald K. Hanson, Shock Tube Techniques, Lecture Note 11, Combution Energy Frontier Research Center of Princeton University, 2013.

[11] Subith S. Vasu, David F. Davidson, Ronald K. Hanson, Jet fuel ignition delay times: Shock tube experiments over wide conditions and surrogate model predictions, Combustion and Flame, 152 (2008), 125-143.

[12] Sandeep Gowdagiri, Weijing Wang, Matthew A. Oehlschlaeger, A shock tube ignition delay study of conventional diesel fuel and hydroprocessed renewable diesel fuel from algal oil, Fuel, 128 (2014), 21-29.

[13] Subith S. Vasu, David F. Davidson, Ronald K. Hanson, Jet fuel ignition delay times: Shock tube experiments over wide conditions and surrogate model predictions, Combustion and flame, 1522008, 21-29.